Supporting information for

Synergistic Assembly of Heavy Metal Clusters and Luminescent Organic Bridging Ligands in Metal-organic Frameworks for Highly Efficient X-ray Scintillation

Cheng Wang,[1,†] Olga Volotskova,[2,†] Kuangda Lu,[1] Moiz Ahmad,[2] Conroy Sun,[2] Lei Xing,[2,*] Wenbin Lin[1,*]

[1]Department of Chemistry, University of Chicago, 929 E 57th St, Chicago, IL 60637, USA

[2]Department of Radiation Oncology, School of Medicine, Stanford University, 875 Blake Wilbur Dr., Stanford, CA 94305, USA

Table of Contents

1. Materials and Methods.

All starting materials were purchased from Aldrich and Fisher Scientific, unless otherwise noted, and used without further purification. ^{1}H NMR spectra were recorded on Bruker NMR 400 NB and 400 DRX Spectrometers at 400 MHz and referenced to the proton resonance resulting from incomplete deuteration of deuterated chloroform (δ 7.26). Thermogravimetric analysis (TGA) was carried out on a Shimadzu TGA-50 equipped with a Pt pan. Powder X-ray diffraction was carried out on a Bruker SMART Apex II CCD-based X-ray diffractometer system equipped with a Cu –target X-ray tube and operated at 1600 watts. Scanning electron microscopy (SEM) was used to image the samples, using a Hitachi 4700 field emission scanning electron microscope. Transmission electron microscopy (TEM) was obtained on a JEOL 100CX-II Transmission Electron Microscope. Nitrogen adsorption experiments were performed

with a Quantachrome Autosorb-1C. Steady-state and time-resolved emission spectra were recorded on an Edinburgh FLS 920 spectrometer.

2. Synthesis of Hf-MOF and Zr-MOF.

2.1. Synthesis of Hf-MOF. 9,10-bis(*p*-benzoic acid)anthracene (H_2**L**) was prepared following a literature procedure.[1] The purity of the synthesized ligand was confirmed by ^{1}H NMR spectroscopy. $HfCl_4$ (16 mg, 0.05 mmol), H_2**L** (21 mg, 0.05 mmol), and trifluoroacetic acid (50 μL, 0.8 mmol) were dispersed in DMF (10 mL), sealed in a vial, and placed in an oven. The temperature was kept at 100 °C for 48 hours. After cooling to room temperature, the resulting solid was isolated by centrifugation, and washed with DMF and methanol repeatedly before being dried under vacuum. Yield: 15 mg (45%).

2.2. Synthesis of Zr-MOF. $ZrCl_4$ (11.5 mg, 0.05 mmol), H_2**L** (21 mg, 0.05 mmol), and trifluoroacetic acid (50 μL, 0.8 mmol) were dispersed in DMF (10 mL), sealed in a vial, and placed in an oven. The temperature was kept at 100 °C for 48 hours. After cooling to room temperature, the resulting solid was isolated by centrifugation, and washed with DMF and methanol repeatedly before being dried under vacuum. Yield: 15 mg (40%).

3. Characterization of Hf-MOF and Zr-MOF.

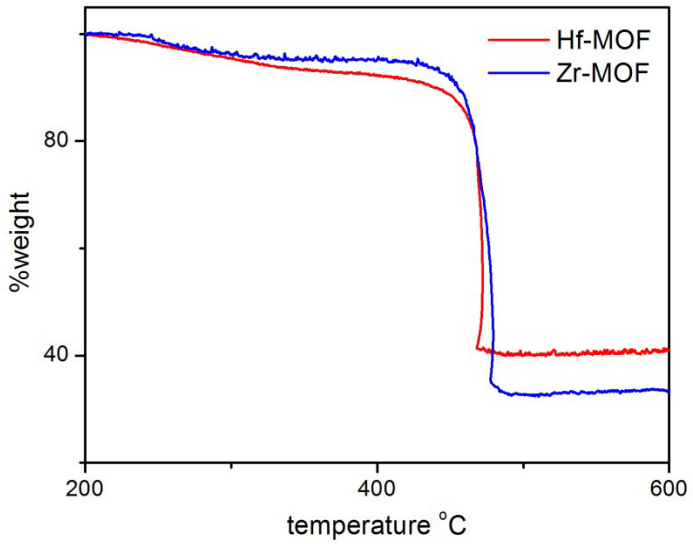

Figure S1.Thermogravimetric analysis (TGA) curves of **Hf-MOF** (red) **and Zr-MOF** (blue).

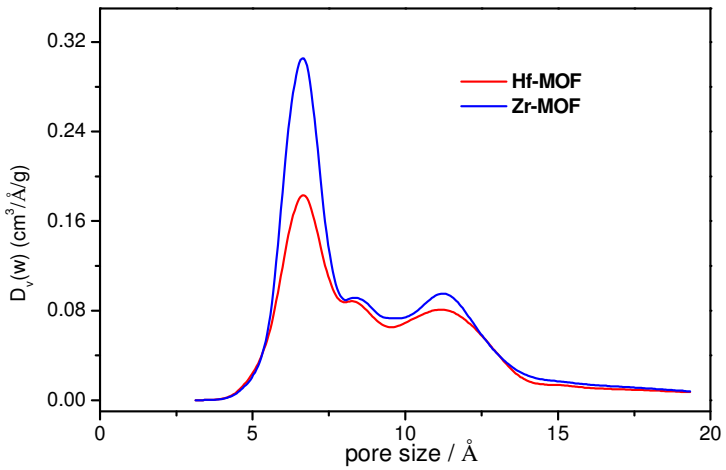

Figure S2. Pore size distributions (HK method) of **Hf-MOF** (red) and **Zr-MOF** (blue) determined from nitrogen uptake measurements at 77 K.

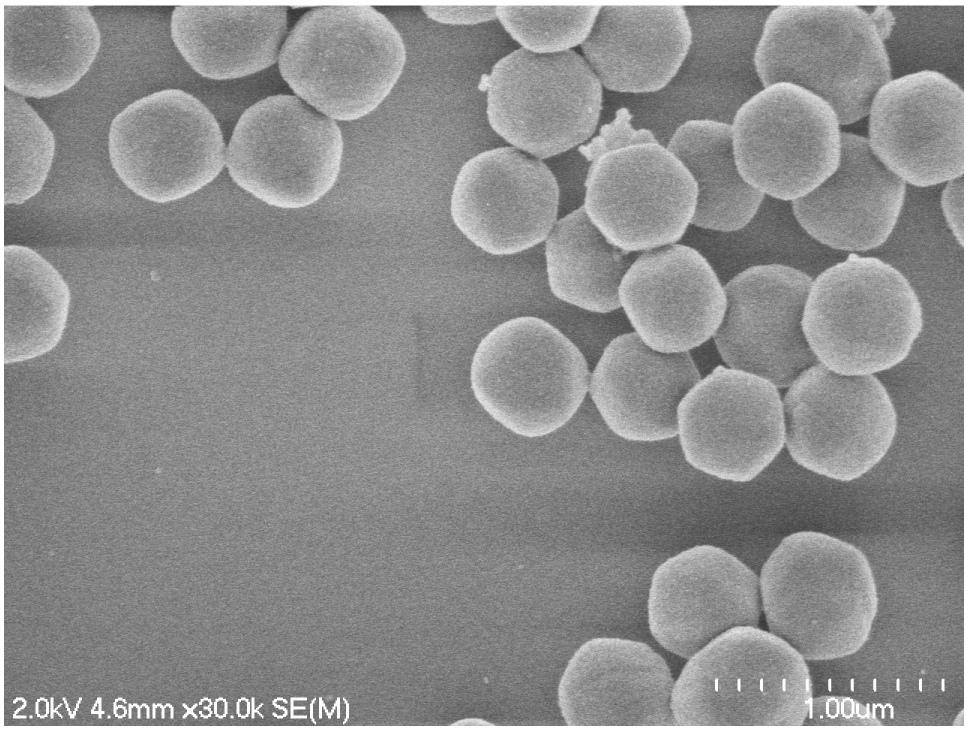

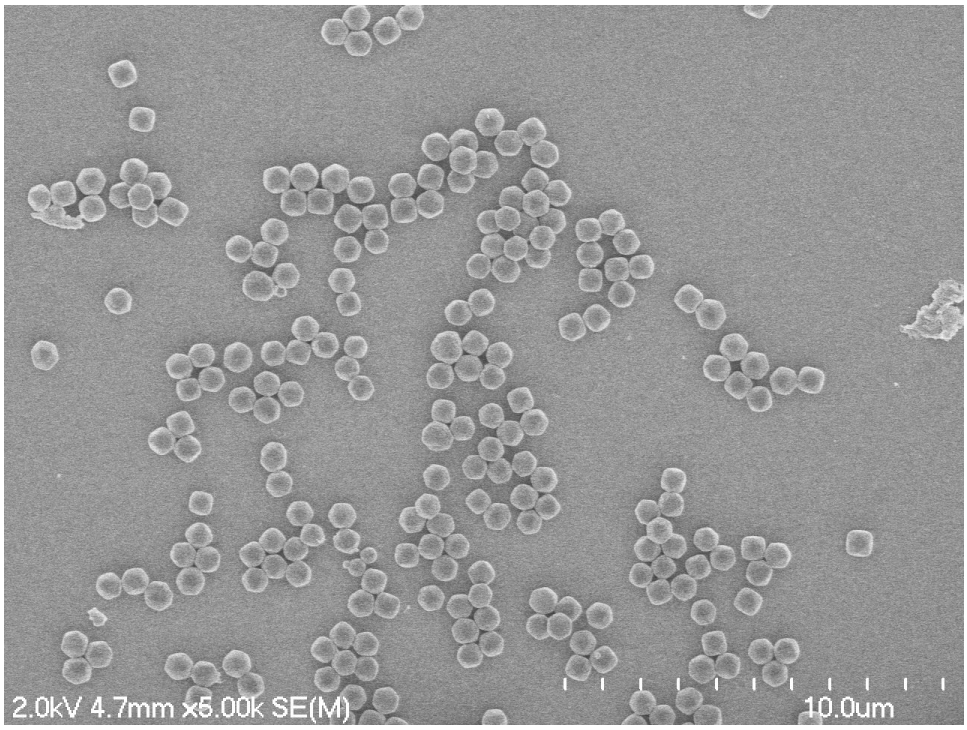

Figure S3. SEM images of **Hf-MOF**.

4. Details of XRD Analysis.

The structural model was built from a published MOF with UiO-type structure, built from Zr and the aminoterphenyldicarboxylate ligand, a linear ligand with the same length as the anthracene ligand.[2] The model adopts the cubic crystal system with Fm-3m space group and lattice parameter of a= 32.7767 Å. The framework is constructed from $M_6(\mu_3\text{-}O)_4(\mu_3\text{-}OH)_4(\text{carboxylate})_{12}$ (M = Hf or Zr) SBU connected by the linear **L** linkers, leading to a **fcu** topology. There is a rotational disorder of the linear anthracene ligand as a result of the rotation of the anthrancene ring with respect to the benzoate rings, a typical structural disorder observed in open-framework MOFs with linear ligands. Such a structural model is supported by the similarity of the experimental PXRD patterns as compared to that theoretically generated from the model (see Figure 2c in the manuscript).

One particular aspect of structural determination of open-channel metal-organic frameworks is that is there catenation in the structure. Structural catenation refers to two or more sets of frameworks interpenetrating into each other to form structure. In the most general case, the structural catenation only has small effects on the PXRD patterns, and is difficult to be identified by PXRD patterns. Fortunately, in the UiO structure, non-interpenetrated structure adopts Fm-

3m space group while 2-fold interpenetrated structure adopts Fd-3m space group.[3] Because of the d glide plane in the interpenetrated structure, it has additional systematic absence of hk0 (h+k=4n). As a result, 200 diffraction will be absent in a 2-fold interpenetrated structure, and will be present in a non-interpenetrated structure, serving as a sensitive probe for catenation in this system. As show in Figure S4, the presence of the 200 peak in the experimental PXRD data clearly indicates the non-interpenetrated structures for Hf-MOF and Zr-MOF.

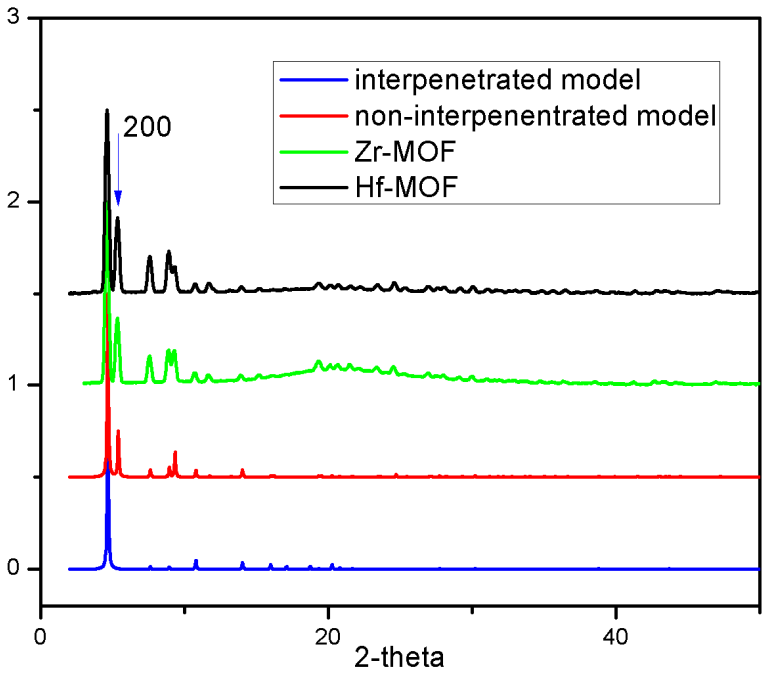

Figure S4. Simulated PXRD patterns from non-interpenetrated (red) vs. interpenetrated (blue) models, together with the experimental patterns of **Hf-MOF** (black) and **Zr-MOF** (green).

5. Fluorescence spectra of Hf-MOF, Zr-MOF, and H_2L.

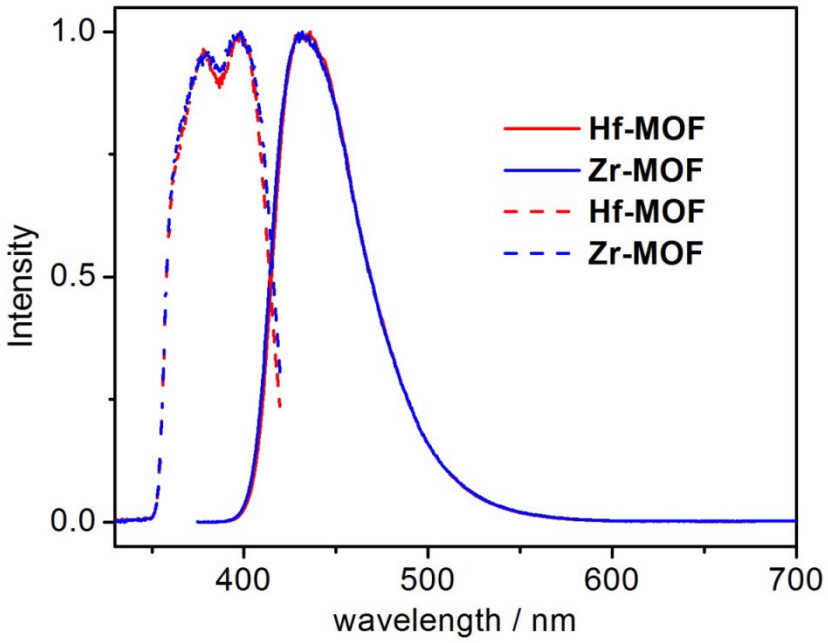

Figure S5. Fluorescent spectra of **Hf-MOF** (red, solid) and **Zr-MOF** (blue, solid) suspensions in DMF (0.04 mM **L**) excited at a wavelength of 368.8 nm, and the corresponding excitation spectra monitored at 469 nm (dashed lines).

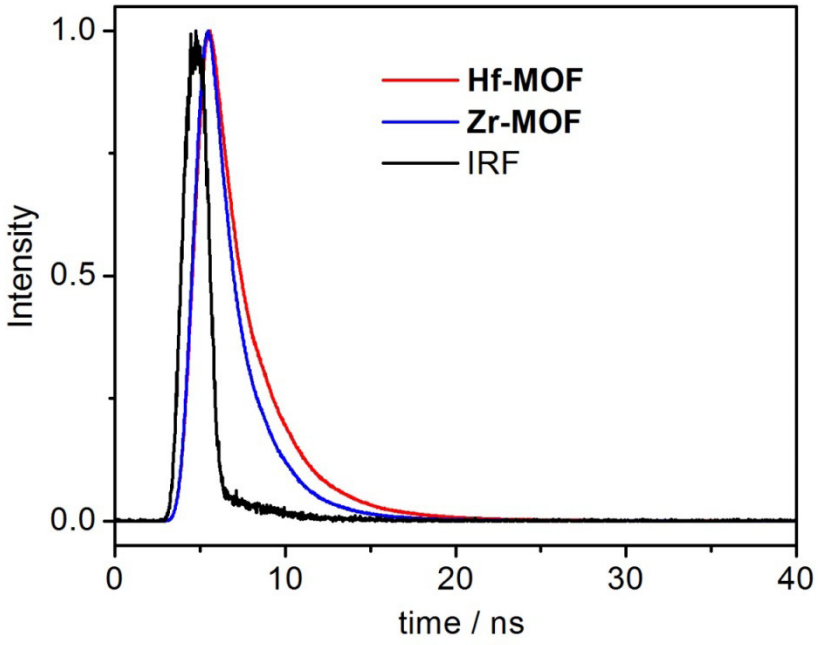

Figure S6. Time-resolved fluorescent decay traces of **Hf-MOF** (red) and **Zr-MOF** (blue) suspensions in DMF excited at 368.8 nm and monitored at 469 nm, together with instrument response function (IRF, black).

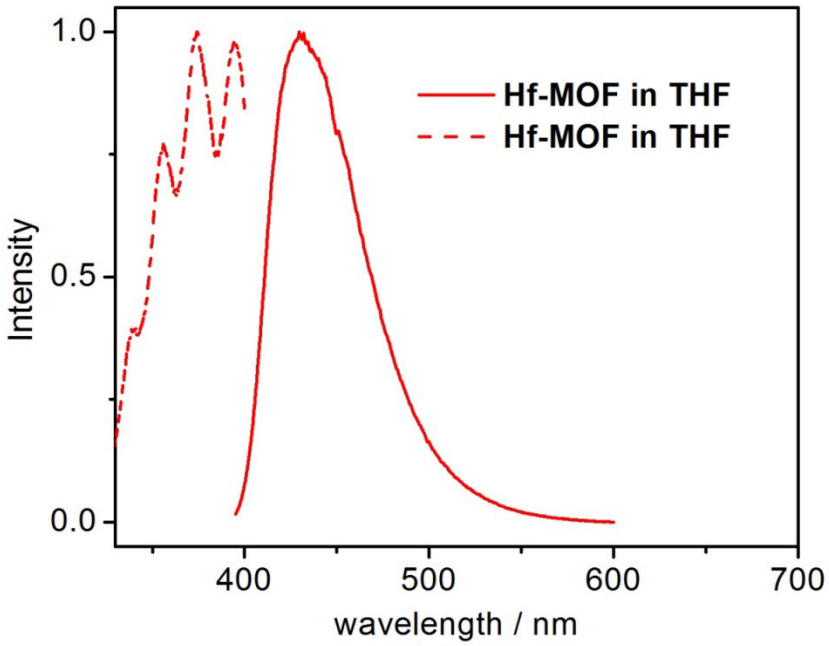

Figure S7. Fluorescent spectra of **Hf-MOF** (red, solid) suspension in THF (0.04 mM **L**) excited at a wavelength of 368.8 nm, and the corresponding excitation spectra monitored at 469 nm (dashed line).

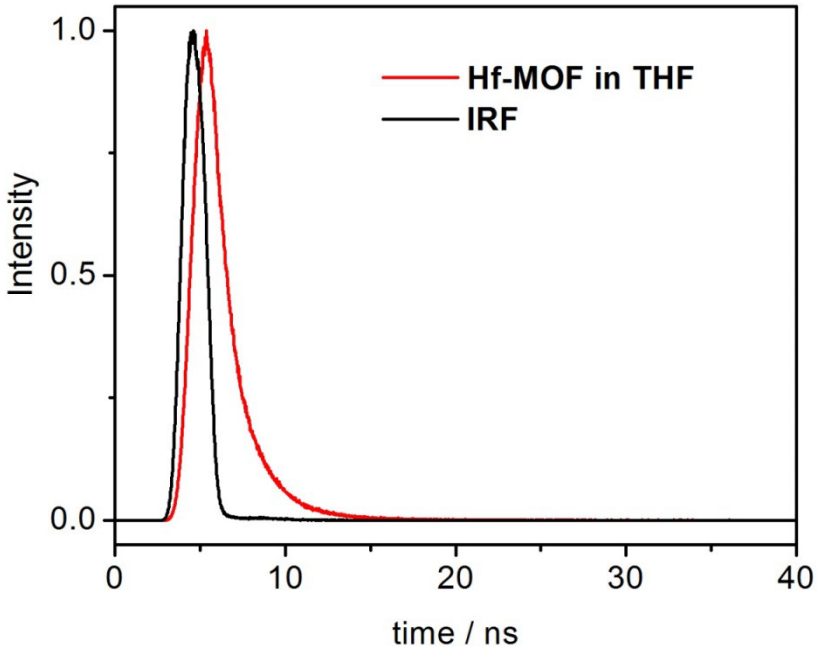

Figure S8. Time-resolved fluorescent decay traces of **Hf-MOF** (red) suspension in THF excited at 368.8 nm and monitored at 431 nm, together with instrument response function (IRF, black).

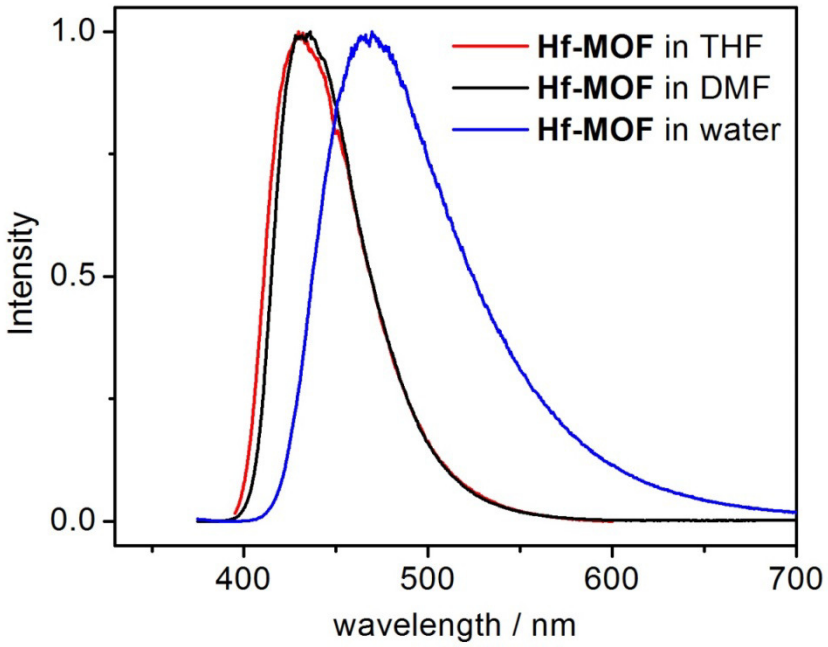

Figure S9. Fluorescent spectra of **Hf-MOF** suspensions in THF (red), DMF (black) and water (blue) excited at 368.8 nm.

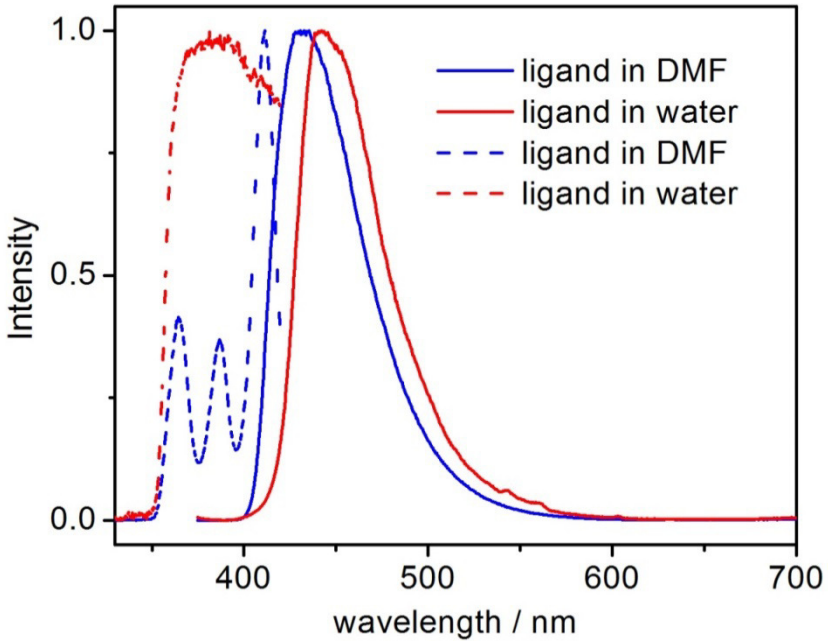

Figure S10. Fluorescent spectra of a DMF solution of 0.04 mM H_2**L** (red, solid) and an aqueous suspension of 0.04 mM H_2**L** insoluble particles (blue solid) excited at a wavelength of 368.8 nm, and the corresponding excitation spectra monitored at 441 nm (dashed lines).

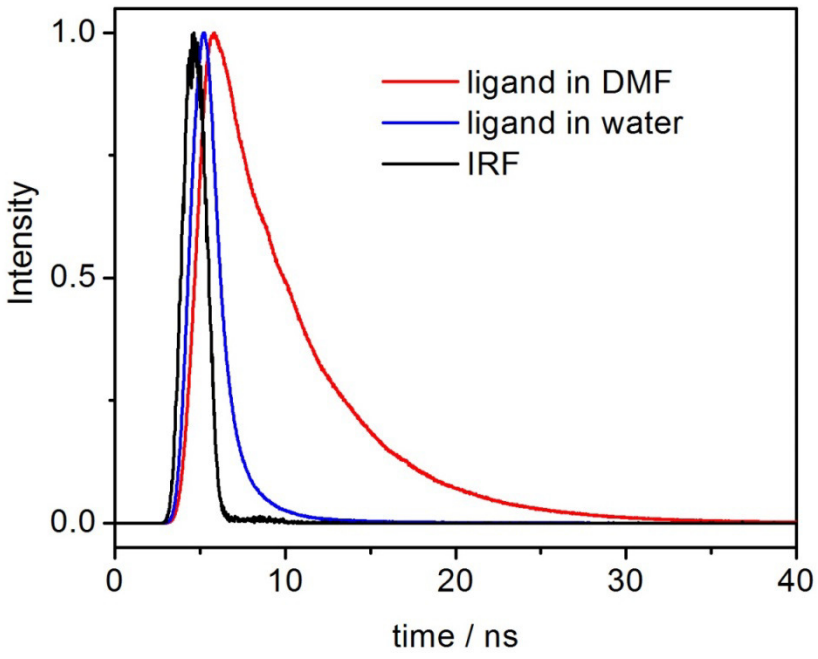

Figure S11. Time-resolved fluorescent decay traces of 0.04 mM H_2**L** (red) and an aqueous suspension of 0.04 mM H_2**L** insoluble particles (blue) excited at a wavelength of 368.8 nm, monitored at 441 nm, together with instrument response function (IRF, black).

6. Fitting of fluorescent decay traces of Hf-MOF, Zr-MOF and H_2L.

The emission decays in of the suspended particles were fit to bi-exponential expression $A = A_1e^{-t/\tau 1} + A_2e^{-t/\tau 2}$. The reported lifetime τ is the weighted lifetime $\tau = (A_1\tau_1^2 + A_2\tau_2^2)/(A_1\tau_1 + A_2\tau_2)$.

Table S1. Fitting of emission decay traces of Hf-MOF, Zr-MOF and H_2L ligand.

Samples	A_1	τ_1 (ns)	A_2	τ_2(ns)	χ^2	τ(ns)
Hf-MOF in H_2O	0.748	5.06±0.04	0.251	8.25±0.12	1.037	6.19±0.07
Hf-MOF in DMF	0.910	2.73±0.01	0.090	8.42±0.08	1.089	4.06±0.03
Hf-MOF in THF	0.888	1.81±0.07	0.111	3.6±0.1	1.122	2.17±0.08
Zr-MOF in H_2O	0.858	5.60±0.01	0.142	7.57±0.02	1.125	5.96±0.01
Zr-MOF in DMF	0.911	2.33±0.01	0.089	8.41±0.09	1.212	3.92±0.03
H_2**L** in H_2O	0.858	0.88±0.05	0.142	3.66±0.08	0.913	2.0±0.1
H_2**L** in DMF	0.227	3.75±0.11	0.773	5.65±0.03	1.314	5.34±0.04

7. X-ray induced fluorescence.

Experimental details of the X-ray luminescence intensity measurements. MOF suspensions in water or ethanol (200 uL of each in a 96 well plate) or solid MOF samples were placed inside the tight-light box and positioned in one row at the distance ~ 30cm from a point X-ray source , or individually in the distance of 1 cm from a point mini X-ray source (mini X Amptek). The data were recorded with an electron-multiplying CCD camera (EM-CCD Hamamtsu, ImageEM C9100-13) cooled at -80C, using ¼f lens, image size 256X256 pixels with an exposure time of 10 sec or 0.01sec and EM gain of 200 or 50 respectively. These different settings were chosen depending on samples' overall brightness. All experiments were repeated at least 3 times. The dose delivered to the samples was measured with Farmer pinpoint ionization chamber (model TN31104). The spectrum of X-ray photons was characterized with x-ray spectrometer Amptek model# X-123CdTe (Fig.S12 S13).

Experimental set-ups of the X-ray luminescence spectrum measurement. The set-up is constructed from an X-ray source (mini–x, Amtek Inc.), a monochromator (Princeton Instruments) and an EM-CCD (Princeton Instruments).

Experimental details of the high dose X-ray stability measurements. Optical stability of the radioluminescence against X-ray damaging was examined: the cumulative dose up to of 300 Gy was delivered to Zr-MOF and Hf-MOF samples by means of linear accelerator (Varian TrueBeam). X-ray luminescence was examined by very low-dose X-ray irradiation (~0.25 uGy, by means of InVivo Extreme Bruker X ray/Optical Imaging System) before and after ultra-high-dose was delivered to samples: no substantial decrease of the X-ray induced luminescence was observed (Fig. S17).

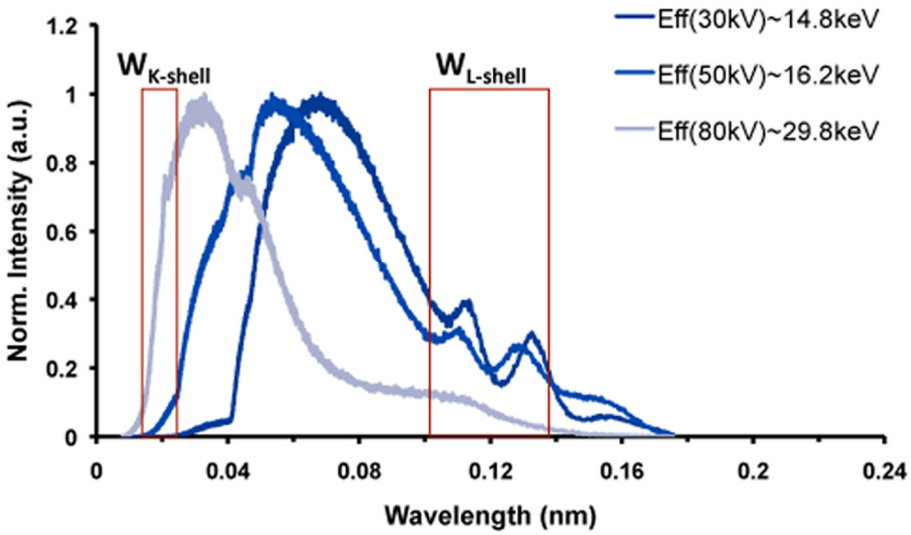

Figure S12. Experimental measurements of X-ray excitation spectra used to induce luminescence (Therapax Series 3) with effective energies 14.8, 16.2 and 29.8 keV for tube voltages 30, 50 and 80kV accordingly.

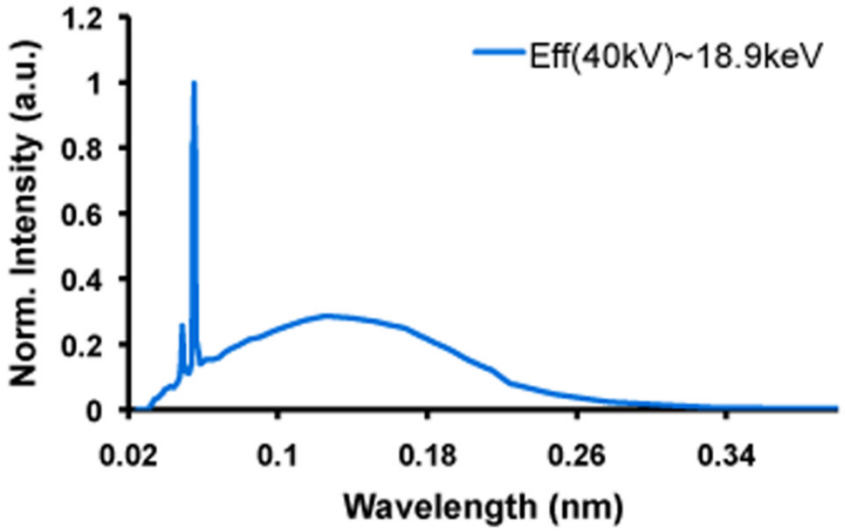

Figure S13. X-ray excitation spectrum of mini X source with effective energy 18.9keV for the tube voltage 40kV.

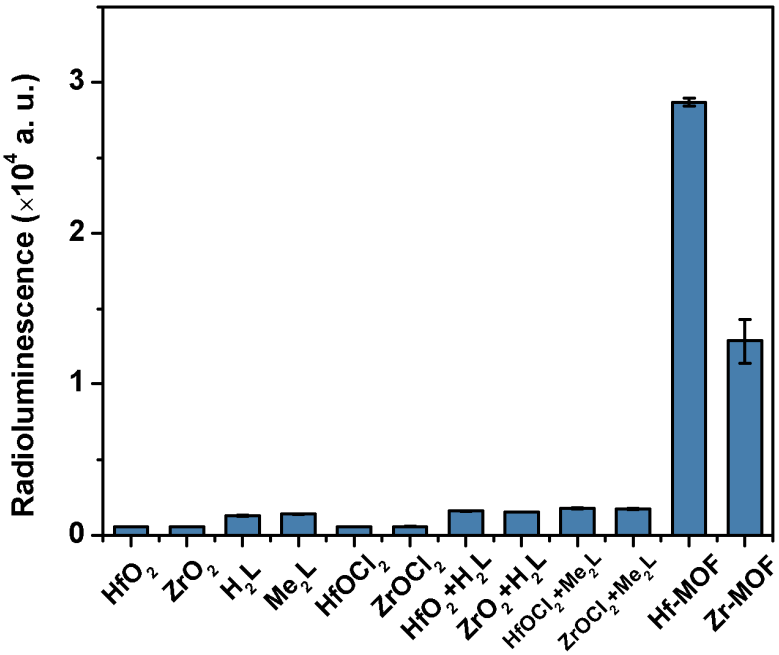

Figure S14. Radioluminescence signals of **Hf-MOF**, **Zr-MOF** and control samples in aqueous suspension/solution: (from left to right) HfO_2 and ZrO_2 colloidal nanoparticles, the anthracene ligand H_2**L** alone, methyl ester of the anthracene ligand Me_2**L**, H_2**L** + HfO_2 colloid and H_2**L** + ZrO_2 colloid, $HfOCl_2$ + Me_2**L**, $ZrOCl_2$ + Me_2**L**, Hf-MOF, Zr-MOF . Measurement conditions: 40 kV tube voltage, 0.08 mA tube current, ~18.9keV effective x-ray energy, 1 Gy / 10 sec, 200 gain.

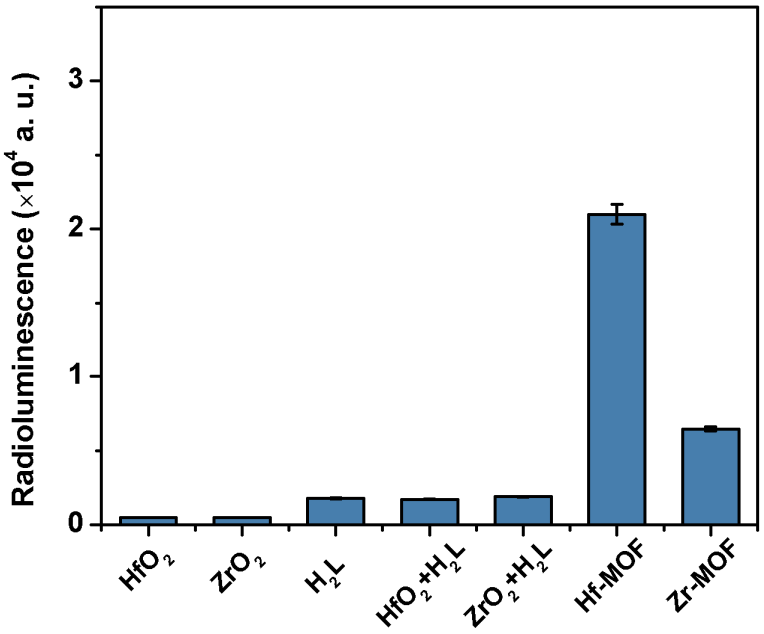

Figure S15. Radioluminescence signals of **Hf-MOF**, **Zr-MOF** and control samples in ethanol suspension: (from left to right) HfO_2 and ZrO_2 colloidal nanoparticles, the anthracene ligand H_2**L** alone, H_2**L** + HfO_2 colloid and H_2**L** + ZrO_2 colloid, Hf-MOF, Zr-MOF. Measurement conditions: 40 kV tube voltage, 0.08 mA tube current, ~18.9keV effective x-ray energy, 1 Gy / 10 sec, 200 gain.

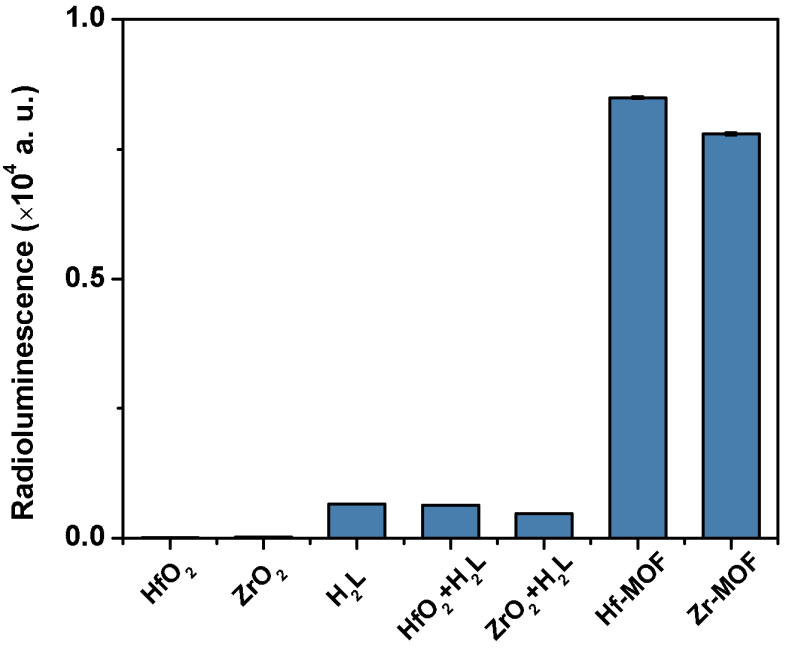

Figure S16. Radioluminescence signals of dry **Hf-MOF**, **Zr-MOF** and solid state control samples: (from left to right) HfO_2 and ZrO_2 colloidal nanoparticles, the anthracene ligand H_2**L** alone, H_2**L** + HfO_2 colloid and H_2**L** + ZrO_2 colloid, **Hf-MOF**, **Zr-MOF**. Measurement conditions: 40 kV tube voltage, 0.08 mA tube current, ~18.9keV effective x-ray energy, 1 mGy / 0.01 sec, 50 gain.

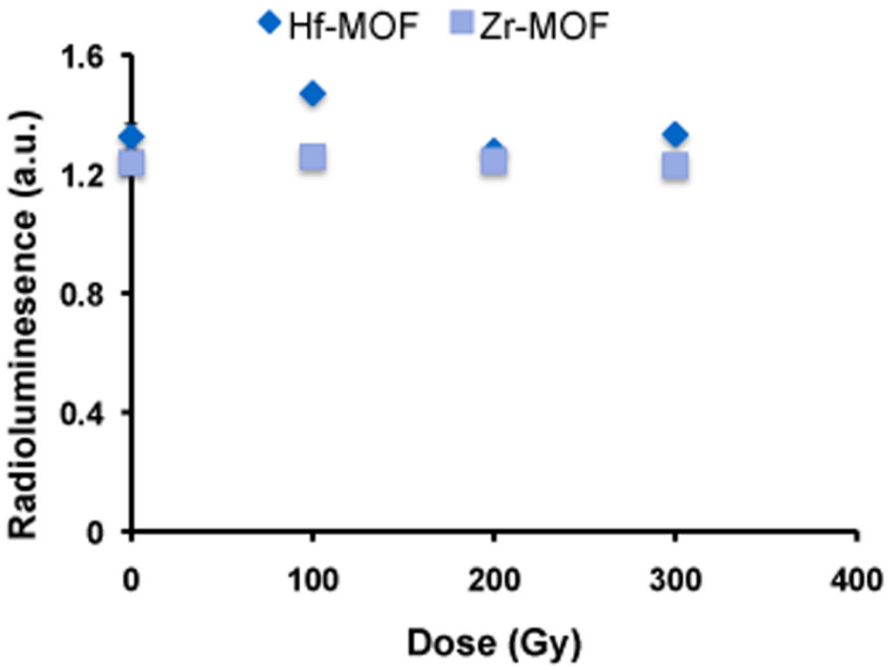

Figure S17. Stability test of **Hf-MOF** and **Zr-MOF**. The radiolumenescence signal was recorded from the same samples before and after high-dose delivery. Low-dose x-ray irradiation (0.25 uGy) was used to detect if any minor changes occur in the optical signal. The signals from MOFs were normalized.

8. References.

(1)Hauptvogel, I. M.; Biedermann, R.; Klein, N.; Senkovska, I.; Cadiau, A.; Wallacher, D.; Feyerherm, R.; Kaskel, S. *Inorganic Chemistry* **2011**, *50*, 8367.

(2) Schaate, A.; Roy, P.; Godt, A.; Lippke, J.; Waltz, F.; Wiebcke, M.; Behrens, P. *Chemistry – A European Journal* **2011**, *17*, 6643.

(3) Andreas Schaate, Pascal Roy, Thomas Preuβe, Sven Jare Lohmeier, Adelheid Godt, Peter Behrens *Chemistry – A European Journal* **2011**, *17*, 9320.